

**COB-2023-2229**

## **CHARACTERIZATION OF THERMOPHYSICAL PROPERTIES OF PHASE CHANGE MATERIALS FOR THERMAL SOLAR ENERGY STORAGE**

**Cristina Isabel Cogollo Torres**  
**Manuel José Osorio Pérez**  
**Arnold Rafael Martínez Guarín**  
**Jorge Mario Mendoza Fandiño**  
**Jesús David Rhenals Julio**  
**Jorge Emilio Rhenals Hoyos**

Department of Mechanical Engineering, University of Córdoba, Carrera 6 No. 77-305 Montería - Colombia. ZIP code 230002  
ccogollotorres@correo.unicordoba.edu.co, majosopez@gmail.com, arnoldrafael@correo.unicordoba.edu.co  
jorge.mendoza@correo.unicordoba.edu.co, jesusrhenalsj@correo.unicordoba.edu.co, jrhenalshoyos@correo.unicordoba.edu.co

**Abstract.** *In this study, phase change materials (PCMs) were characterized for their use in thermal energy storage systems. Economical characterization methods were employed to determine the thermophysical properties of PCMs available in the Colombian market. The T-History and T-Melting (CHF) methods were used to determine the melting point, enthalpy of fusion, thermal conductivity, and specific heat capacity of the PCMs. The results obtained through the T-History method showed acceptable error percentages in the measured properties. However, estimating the specific heat capacity in the solid state proved challenging due to difficulties in accurately assessing area differences at close temperatures. On the other hand, the CHF method encountered difficulties in calculating the specific heat capacity in the liquid state due to heat losses in the test module. Comparison with internationally used paraffins as reference materials demonstrated that Colombian PCMs exhibit comparable thermophysical properties and show potential for thermal energy storage. These findings represent a significant advancement in the national understanding of PCMs and their application in thermal energy storage systems. In conclusion, this study successfully characterized Colombian PCMs using economical characterization methods, providing relevant information for their implementation in thermal energy storage systems. The obtained results demonstrate the potential of these materials for such applications and contribute to the state of the art in PCM research in Colombia.*

**Keywords:** *Phase Change Materials, Thermal Energy Storage, Thermophysical Properties, Characterization Methods.*

### **1. INTRODUCTION**

In recent years, meeting the global demand for energy supply has proven to be a major challenge, leading to the development of sustainable and environmentally friendly energy sources (Midilli et al., 2007). In this regard, solar energy stands out as an attractive option; however, it has high intermittency and requires high maintenance costs (Koshti et al., 2023). Therefore, it is necessary to develop thermal energy storage (TES) systems that reduce costs and increase the efficiency of these devices, bridging the gap between energy supply and demand and achieving competitive systems in the energy market (Mahdi et al., 2019).

The two most common storage systems are sensible heat storage (SHS) and latent heat storage (LHS). The latent heat storage system is the most attractive due to the advantages of its high storage density and its isothermal characteristics. (Mayilvelnathan et al., 2019). LHS (Latent Heat Storage) systems use phase change materials (PCM) as a medium for thermal energy storage. PCM refers to materials characterized by high latent heat, which means they can store or release large amounts of heat during a phase change. This solution allows for a higher amount of heat to be stored in a fixed volume, which can be utilized in cooling or heating applications (Raccanello et al., 2019).

The implementation of PCM is due to its high energy density and its isothermal behavior during charging and discharging. The selection of the appropriate PCM for a latent heat storage system is as complex as it is necessary, making it essential to measure the thermal properties of these materials. (Dincer, 2002).

A good phase change material must meet thermodynamic criteria to be considered viable. One of the main criteria is to have a high value of fusion enthalpy ( $H_m$ ) because the purpose is to store heat, and the more heat stored, the better the material. It should also have an appropriate melting point ( $T_m$ ). If the material does not have a melting point within the desired temperature range, it may not be suitable for the application. Additionally, a high thermal conductivity ( $k$ ) is needed. Materials with high thermal conductivity allow for quick heating and cooling, facilitating efficient energy input and output (Agyenim et al., 2010).

Conventional thermal characterization of materials is typically performed using thermal analysis techniques (Mayayo, J. 2012). Differential scanning calorimetric (DSC) is the most commonly used technique for the thermophysical analysis of PCM. It provides precise information about enthalpy and specific heat at phase change temperatures. However, it has significant limitations: the instrument used is complex and expensive, making it difficult for some researchers or laboratories to access; it requires a very small amount of sample, typically between 1 and 30 mg, to obtain accurate results. In practice, bulk PCM is often used in volumes ranging from cubic centimeters to cubic meters (Jin et al., 2014). It's important to note that the properties of such a small sample may differ from those of bulk samples, which can introduce certain variations and limitations when extrapolating results obtained with differential scanning calorimetric to large-scale PCM systems (Dumas et al., 2014).

Among the newly developed methods is the T-History, which was proposed by Zhang and Jiang in 1999. This method is capable of simultaneously measuring the fusion latent heat, specific heat capacity, and thermal conductivity of various bulk PCM samples. The test is based on monitoring the temperature curves of the PCM sample and a well-known reference sample (usually distilled water) during their natural cooling process. The grouped capacity method is used to analyze the process, and the corresponding thermophysical properties can be determined (Zhang et al., 1999). Compared to conventional DSC methods, this method simplifies the testing instrument, thereby reducing costs considerably (Zhang et al., 1999).

Another developed method is T-Melting CHF, proposed by Xiao-Hu Yang and Jing Liu in 2018. It is capable of determining the melting point, fusion latent heat, thermal conductivity, and specific heat capacity in both solid and liquid phases (Yang et al., 2018). The method monitors the temperature response of the PCM sample during its melting process under constant heat flux conditions. The heat flux conditions are achieved by applying constant heating power, making the measuring apparatus simpler than traditional methods as all the thermophysical properties are determined simultaneously (Yang et al., 2018).

In this study, the T-History and T-Melting CHF methods were replicated, starting with the construction of the necessary devices and their validation. The aim was to identify the thermal conductivity, fusion enthalpy, specific heat capacity, phase change temperature, and density in the liquid and solid states, with the goal of implementing them in thermal solar energy utilization applications.

## 2. MATERIALS AND METHODS

The phase change materials selected as reference samples for this study were Rubitherm® RT45 and RT55 paraffins, which are certified with RAL, the standard for materials used in thermal energy storage applications. Additionally, two commercially available paraffins were characterized: a light and medium-grade paraffin produced in Colombia, and another from Taiwan available in the local market. These paraffins were used in the experiments under the same conditions as received, meaning they were not subjected to purification processes.

### 2.1 T-History Method

This method is based on comparing the temperature evolution of the material under test with that of another reference material with known thermophysical properties. The studied samples and the reference samples were subjected to a cooling process in a controlled chamber, contained in containers that ensure a Bi number  $< 0.1$  to validate the assumption of one-dimensional heat transfer. This allows for the estimation of thermophysical properties by comparing the areas under the curves of the process between the two materials (Zhang et al., 1999).

#### 2.1.1. Measurement Principle

A tube containing a phase change material with a uniform temperature  $T_0$ , which is higher than the melting point of the PCM, is exposed to an atmosphere with a temperature  $T_{\infty,a}$  the resulting curve obtained during this process is known as the T-History curve. When the Biot number (Bi) is less than 0.1, the temperature distribution in the sample is considered to be uniform, allowing the use of the lumped capacitance method. First, we have equation 1:

$$(m_t c_{p,t} + m_p c_{p,l})(T_0 - T_s) = hA_c A_1 \quad (1)$$

For this equation,  $m_p$  y  $m_t$  the masses of the PCM and the tube are represented,  $c_{p,l}$  y  $c_{p,t}$  represent the average specific heats of the liquid PCM and the tube, respectively,  $A_c$  represents the convective heat transfer area of the tube, and  $A_1 = \int_0^{t_1} (T - T_{\infty,a}) dt$ .

Additionally, the following equations should also be considered 2 and 3:

$$m_p H_m = hA_c A_2 \quad (2)$$

Where  $H_m$  is the fusion heat of the PCM and  $A_2 = \int_{t_1}^{t_2} (T - T_{\infty,a}) dt$ . The time interval between  $t_1$  and  $t_2$  represents the duration of the phase change process.

$$(m_t c_{p,t} + m_p c_{p,s})(T_s - T_r) = hA_c A_3 \quad (3)$$

In which  $c_{p,s}$  is the average specific heat of the solid PCM,  $A_3 = \int_{t_2}^{t_3} (T - T_{\infty,a}) dt$  and  $T_r$  is the temperature of the reference substance.

Now, considering a tube filled with pure water and exposed to the same conditions mentioned earlier, equations 4 and 5 are proposed:

$$(m_t c_{p,t} + m_w c_{p,w})(T_0 - T_s) = hA_c A'_1 \quad (4)$$

$$(m_t c_{p,t} + m_w c_{p,w})(T_0 - T_r) = hA_c A'_2 \quad (5)$$

Where  $m_w$  is the mass of the water and  $c_{p,w}$  is the average specific heat of water,  $A'_1 = \int_0^{t'_1} (T - T_{\infty,a}) dt$  y  $A'_2 = \int_0^{t'_2} (T - T_{\infty,a}) dt$ .

From equations (1) to (5), equations 6, 7 and 8 can be obtained:

$$c_{p,s} = \frac{m_w c_{p,w} + m_t c_{p,t}}{m_p} \frac{A_3}{A'_2} - \frac{m_t}{m_p} c_{p,t} \quad (6)$$

$$c_{p,l} = \frac{m_w c_{p,w} + m_t c_{p,t}}{m_p} \frac{A_1}{A'_1} - \frac{m_t}{m_p} c_{p,t} \quad (7)$$

$$H_m = \frac{m_w c_{p,w} + m_t c_{p,t}}{m_p} \frac{A_2}{A'_1} (T_0 - T_s) \quad (8)$$

By using these equations, it is possible to obtain the specific heat of the phase change material in its solid and liquid phases, as well as its phase change energy.

For non-undercooled PCMs, where the temperature range of the phase change process is between  $T_{m,1}$  and  $T_{m,2}$ , the expressions for  $c_{p,l}$  and  $c_{p,s}$  remain the same as mentioned earlier. However, the fusion heat is defined in equation 9:

$$H_m = \frac{m_w c_{p,w} + m_t c_{p,t}}{m_p} \frac{A_2}{A'_1} (T_0 - T_{m,1}) - \frac{m_t c_{p,t} (T_{m,1} - T_{m,2})}{m_p} \quad (9)$$

Both materials must be contained in containers with the same geometry to ensure the same heat transfer coefficient and enable consideration of the heat transfer. Figure 1 shows a schematic diagram of the experimental setup for this method (Zhang et al., 1999).

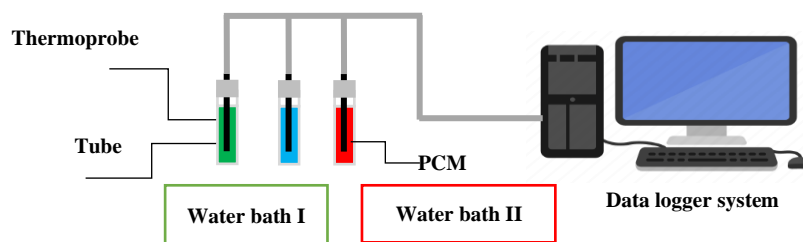


Figure 1. Schematic diagram of the T-History method.

As a variation to the original method and aiming to reduce uncertainties associated with the convection coefficient value around the sample, expanded polystyrene insulation was used. The purpose was to achieve a significantly lower

conduction resistance within the tubes compared to the convection resistance through the fluid boundary layer, ensuring a uniform temperature distribution within the sample.

### 2.1.2. Experimental Conditions

The resulting cooling curves for both the reference material and the PCM were loaded into a script that contains the equations of the method for estimating the thermophysical properties. The temperature range for data evaluation was determined by calculating the derivative of the curves, thereby establishing the inflection points that would mark the phase change region. However, the obtained data exhibited high levels of noise, necessitating the use of a filter to reduce signal noise for improved analysis. Table 1 describes the basic operating conditions of the tests.

Table 1. T-History Test Conditions

PCM	Water mass (g)	PCM mass (g)	Density $\delta L$ (kg/m <sup>3</sup> )
RT-45	15.29	12.33	770.00
RT-55	15.66	12.80	770.00
Col TW	16.74	12.29	780.78
Light	17.11	12.30	762.40
Medium	17.11	12.66	771.58

The samples were packed in test tubes with a 15 mm diameter and 150 mm height, featuring a side release, and sealed hermetically with a cork. To determine the mass, a digital balance was used. The test temperature was measured using an 8-channel digital thermometer and 4 type K thermocouples, which were vertically positioned in the center of the tubes. The samples were heated in a water bath, and the cooling process was conducted in an expanded polystyrene (EPS) chamber. The test tubes were placed in 3 EPS compartments to prevent convective effects around the tubes, as shown in Figure 2. The experiment was concluded when the samples reached room temperature.

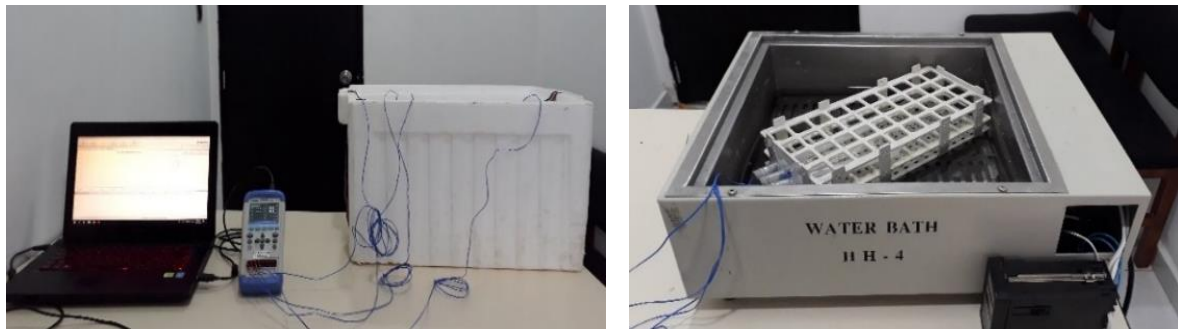


Figure 2. Experimental setup of the T-History method

## 2.2. T-Melting CHF Method

This method is capable of simultaneously determining the key thermophysical properties of PCM, such as melting point, latent heat, thermal conductivity, and specific heat capacity in both solid and liquid phases, in a single test (Yang et al., 2018).

### 2.2.1. Measurement Principle

Assuming the test module is perfectly insulated, Figure 3 schematically represents a typical monitoring temperature curve ( $T_{mon}$ ). The curve can be divided into three processes: the pre-melting process, the melting process, and the post-melting process.  $T_{ref,1}$  is the inflection point at which the PCM starts to melt, occurring at the time denoted as  $t_1$ , and the melting process concludes at  $t_2$  (Yang et al., 2018).

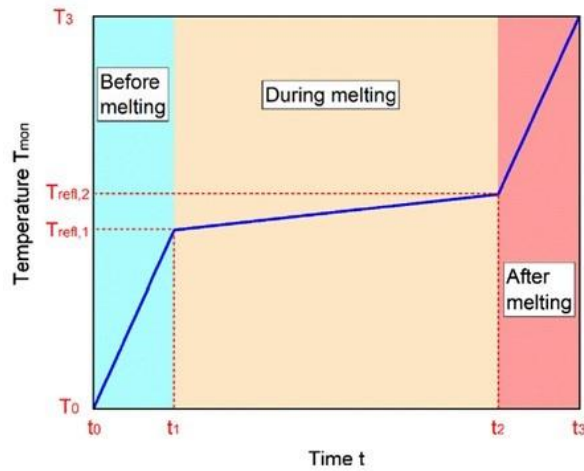


Figure 3. Schematic of a typical temperature response curve  $T_{mon}$  with a constant heating power  $q_{hs}$

According to the model, the melting point of the PCM can be obtained using the following equation 10:

$$T_m = T_{refl,1} - \frac{q_{hs} L_{Al}}{A_{hs} K_{Al}} \quad (10)$$

The law of energy conservation can be applied to the three processes using equations 11, 12, and 13.

Before melting:

$$q_{hs} = (m_{hs} C_{p,hs} + m_{Al} C_{p,Al} + m_{PCM} C_{p,s,PCM}) \frac{dT}{dt} \Big|_{be-m} \quad (11)$$

After melting:

$$q_{hs} = (m_{hs} C_{p,hs} + m_{Al} C_{p,Al} + m_{PCM} C_{p,l,PCM}) \frac{dT}{dt} \Big|_{af-m} \quad (12)$$

During melting:

$$q_{hs} = \left( m_{hs} C_{p,hs} + m_{Al} C_{p,Al} + \frac{1}{2} m_{PCM} C_{p,l,PCM} \right) \frac{dT}{dt} \Big|_{du-m} \quad (13)$$

Where  $m_i C_{p,i}$  ( $i = hs, Al$  o  $PCM$ ) is the heat capacity of the heat source (heater),  $q_m$  is the heat absorbed by the PCM in the form of latent heat. It should be noted that in the equation during fusion, only half of the heat capacity of the liquid PCM is considered. This is because the liquid fraction of the PCM changes from 0 to 1 throughout the fusion process, allowing us to estimate the average heat capacity of the liquid phase to be  $0.5 m_{PCM} C_{p,l,PCM}$ .

The specific heat capacity of the PCM in the solid phase ( $C_{p,s}$ ) and in the liquid phase ( $C_{p,l}$ ) can be obtained using the energy equations before and after fusion, respectively. The energy equation during fusion provides the value of  $q_m$ , which can be used to determine the latent heat of fusion  $\Delta H$ , using equation 14.

$$\int_{t_1}^{t_2} q_m dt = m_{PCM} \Delta H \quad (14)$$

In the model, after performing a theoretical analysis, it was demonstrated that the wall temperature  $T_w$  increases almost linearly with time, and the rate of increase is given by:

$$\frac{dT}{dt} \Big|_{du-m} = \frac{(q_m/A_{hs})^2}{\rho_{l,PCM} K_{l,PCM} \Delta H} \quad (15)$$

Equation 15 states that once the density of the liquid phase of the PCM ( $\rho_{l,PCM}$ ) is known, its thermal conductivity  $K_l$  can be calculated.

The following parameters are required prior to measurement: the geometrical size of the test module, the thermal capacity of the heater ( $m_{hs} C_{p,hs}$ ) and the aluminum plate ( $m_{Al} C_{p,Al}$ ), the mass  $m_{PCM}$  and the density of the liquid phase

$\rho_l$  of the PCM. With the real-time heating power  $q_{hs}$  and the monitored temperature  $T_{mon}$ , the melting point  $T_m$ , the latent heat of fusion  $\Delta H$ , the thermal conductivity in the liquid phase  $K_l$ , and the specific heat capacity  $C_p$  in both solid and liquid phases of the PCM can be determined.

### 2.2.2. Experimental conditions

For the construction of the measurement device, the proposed model in the T-Melting CHF method was replicated, which consists of a test module based on a one-dimensional melting process under constant heat flux conditions (Yang et al., 2018).

Taking into account the limitations of the method, it was necessary to determine the critical heat flux for conducting the experiments. Considering that the PCM to be analyzed is paraffin, an ideal thermal conductivity value of  $0.2 \text{ W/m}^\circ\text{C}$  was assumed, with a sample thickness of  $0.005 \text{ m}$ , an ambient temperature of  $20^\circ\text{C}$ , and a melting temperature of  $90^\circ\text{C}$ . Therefore, the critical heat flux ( $q''$ ) is calculated to be  $2800 \text{ W/m}^2$ . The table shows the conditions under which the experiments were conducted. It can be observed that all tests were performed with heat flux values below the critical heat flux, ensuring that heat transfer in the experiments occurs by conduction. Additionally, the Rayleigh number for each test is below the limit value ( $Ra_c=2.72 \times 10^4$ ), further confirming that heat transfer is dominated by conduction. The table also includes the Stefan number (Ste) for each case.

Table 2. Experimental conditions for T-Melting CHF tests

PCM	Mass of PCM (g)	Heating power $q_{hs}$ (W)	Heat flux $q''$ ( $\text{W/m}^2$ )	Ste	Ra
RT-45	12.56	2.00	1000	0.38	208.23
RT-55	14.39	2.70	1350	0.48	281.11
Col TW	11.90	3.50	1750	0.75	472.32
Light	14.32	3.50	1750	0.49	171.90
Medium	14.46	2.70	1350	0.39	189.67

In compliance with the model's constraints, the test module was constructed using ABS material with a thermal conductivity of  $K=0.17 \text{ W/mK}$  and a melting temperature of  $T_m=100^\circ\text{C}$ , which are suitable characteristics for analyzing the proposed paraffins. The module was 3D printed with a 100% infill. The heat source used was a 50 mm diameter heater with a thickness of 2 mm, a resistance of  $616 \Omega$ , and a maximum heating power of 70 W, as shown in Figure 4.

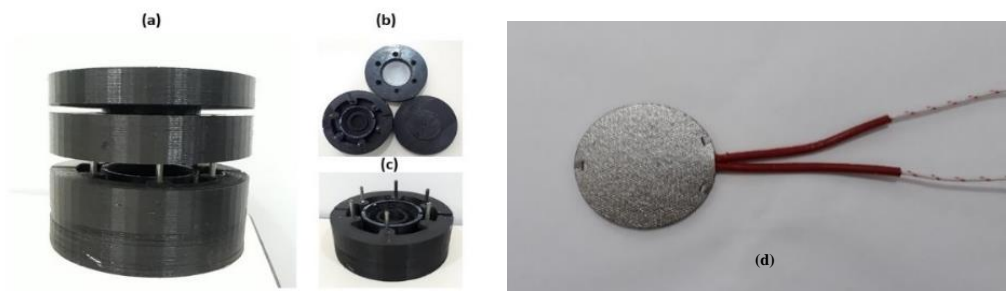


Figure 4. Structure of the constructed test module. (a) Front view, (b) Top view of the base, frame, and lid, (c) Base, (d) Heater used in the test module.

### 2.3. Differential Scanning Calorimetric (DSC)

Differential Scanning Calorimetric (DSC) is a dynamic experimental technique that allows the determination of the amount of heat absorbed or released by a substance when it is maintained at a constant temperature, cooled or heated at a specified rate, within a certain temperature range (Peñalosa, 2016).

For the tests, the Discovery DSC 250 equipment (Figure 5) was used. At the beginning of the experimentation process, the mass of the sample to be analyzed was measured using a precision balance. The sample was weighed inside an aluminum crucible, and once the sample mass value was obtained, the crucible was sealed hermetically using a press.



Figure 5. Experimental setup for the differential scanning calorimetric (DSC) test.

Next, the parameters for the test were established. In terms of the heating and cooling rate, the ASTM D4419-90 standard was followed, which recommends a cooling and heating rate of  $10^{\circ}\text{C}/\text{min} \pm 1$  and a temperature of  $20^{\circ}\text{C} \pm 5$  above the melting point (American et al., 2000).

### 3. RESULTS AND DISCUSSION

#### 3.1. Experimental Evaluation: T-History Method

In Table 3, the values of the thermophysical properties obtained through the T-History Method can be observed.

Table 3. Thermophysical Properties Method: T-History

PCM	Phase Change ( $^{\circ}\text{C}$ )		Hm (kJ/kg)	Cpl (kJ/kg $^{\circ}\text{C}$ )	Cps (kJ/kg $^{\circ}\text{C}$ )
	T initial	T final			
RT-45	44.52	34.78	162.05	2.23	4.35
RT-55	54.51	42.82	168.30	2.44	5.36
Col TW	57.76	46.45	189.70	2.76	5.38
Light	53.73	40.87	185.19	2.99	6.210
Medium	57.62	46.47	186.045	2.54	5.55

The results obtained compared to the manufacturer's data show an average error of 3.79% for the initial point of the phase change region, 18.30% for the final point, 1.14% for the fusion enthalpy, and 16.62% for the liquid specific heat capacity. However, the solid specific heat capacity has a high error of 142.93%. This high error can be explained by the difficulty in accurately evaluating the differences in the area when the reference, the environment, and the sample have very similar temperatures. The above results demonstrate that the method used cannot be used to determine this last property, but it is applicable for the determination of the other properties.

From the obtained results, the Light, Medium, and Taiwanese paraffins prove to be promising phase change materials. They exhibit high energy storage density, around 180 kJ/kg. These values, along with the high specific heats of around 2.5 kJ/kg $^{\circ}\text{C}$ , are sufficiently good to justify further research.

#### 3.2. Experimental Evaluation: T-Melting CHF Method

In Table 4, the values of the thermophysical properties obtained through the T-Melting CHF method can be observed.

Table 4. Thermophysical Properties Method: T-Melting CHF

PCM	Phase Change ( $^{\circ}\text{C}$ )		Cpl (kJ/kg $^{\circ}\text{C}$ )	Cps (kJ/kg $^{\circ}\text{C}$ )	Hm (kJ/Kg)	K (W/mK)
	T initial	T final				
RT-45	37.46	45.72	17.54	2.16	157.17	0.24
RT-55	44.49	57.79	24.41	2.62	175.29	0.20
Col TW	48.05	58.82	35.72	2.81	187.40	0.21
Light	44.49	55.95	23.01	4.30	178.53	0.36
Medium	45.44	59.64	25.01	5.47	194.08	0.27

The obtained results are compared to those reported in the technical datasheets. In the initial melting point, an average error of 13.45% is observed among the samples, while in the final melting point, the error is 1%. The value of  $C_{ps}$  shows an error of 19.54%, the fusion enthalpy exhibits an error of 2.44%, the thermal conductivity has an error of 9.34%, and the value of  $C_{pl}$  shows a high error of 948.8%. The test results indicate that the replicated method has good capability to evaluate the major thermophysical properties of bulk PCM, with the exception of  $C_{pl}$ , which shows a significantly high percentage of error.

### 3.3. Experimental Evaluation: DSC

Using a DSC at a cooling rate of 5 °C/min, the enthalpy and melting point of the RT 45 and RT 55 paraffin samples were determined. For the commercial paraffin samples, heating and cooling curves were performed at a rate of 10 °C/min, and the enthalpy and melting point were similarly determined. In all cases, a single replicate was performed with an average mass of 5 mg. The obtained curves are shown in Figures 6, 7, and 8, and the calculated properties are summarized in Table 3.

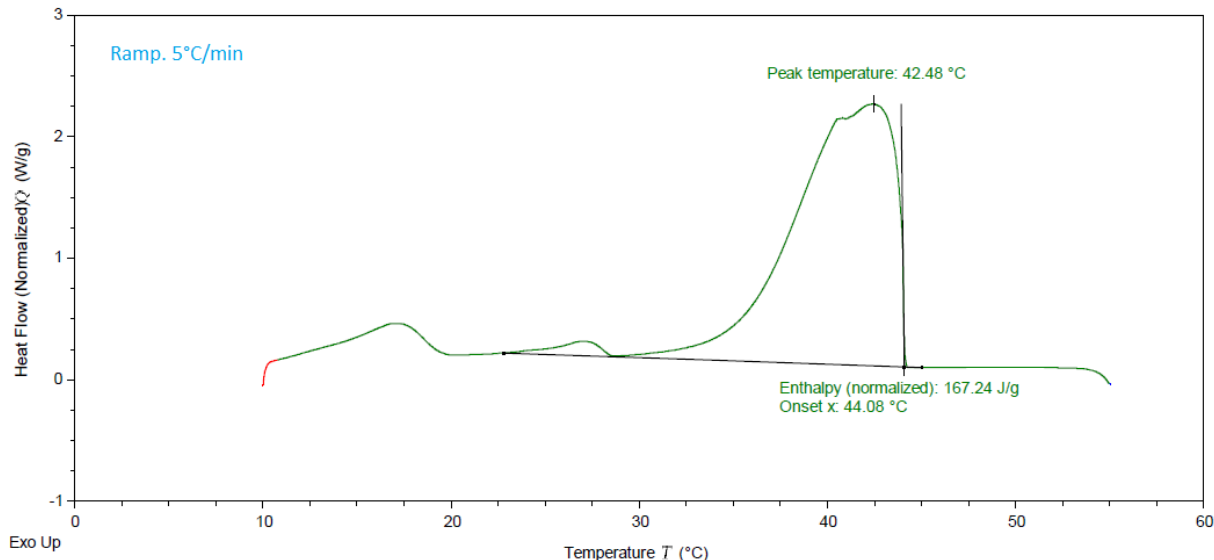


Figure 6. DSC curve performed at 5 °C/min for RT 45 paraffin.

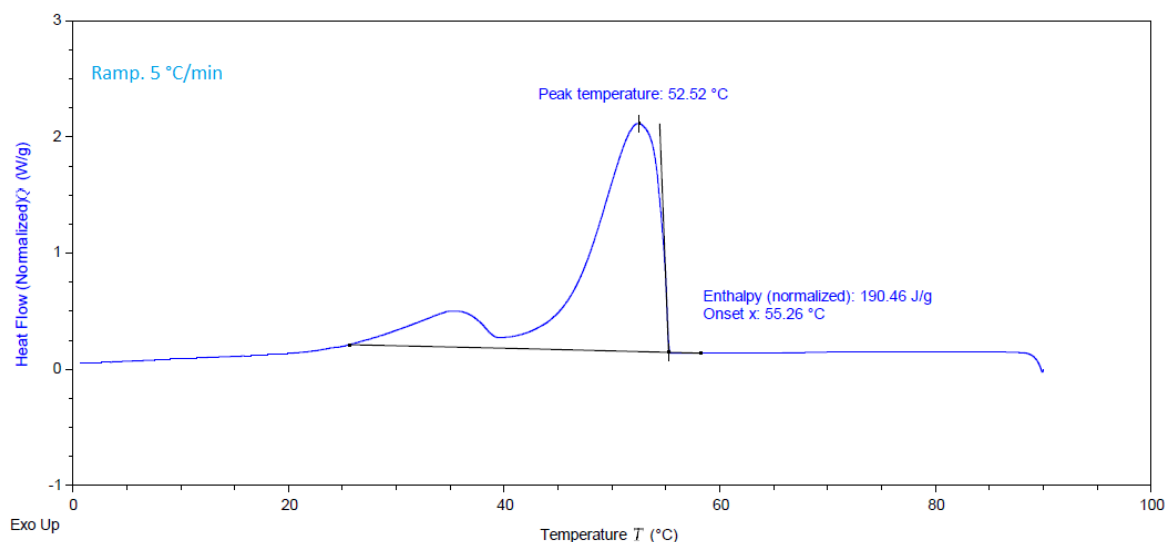


Figure 7. DSC curve performed at 5 °C/min for RT 55 paraffin.

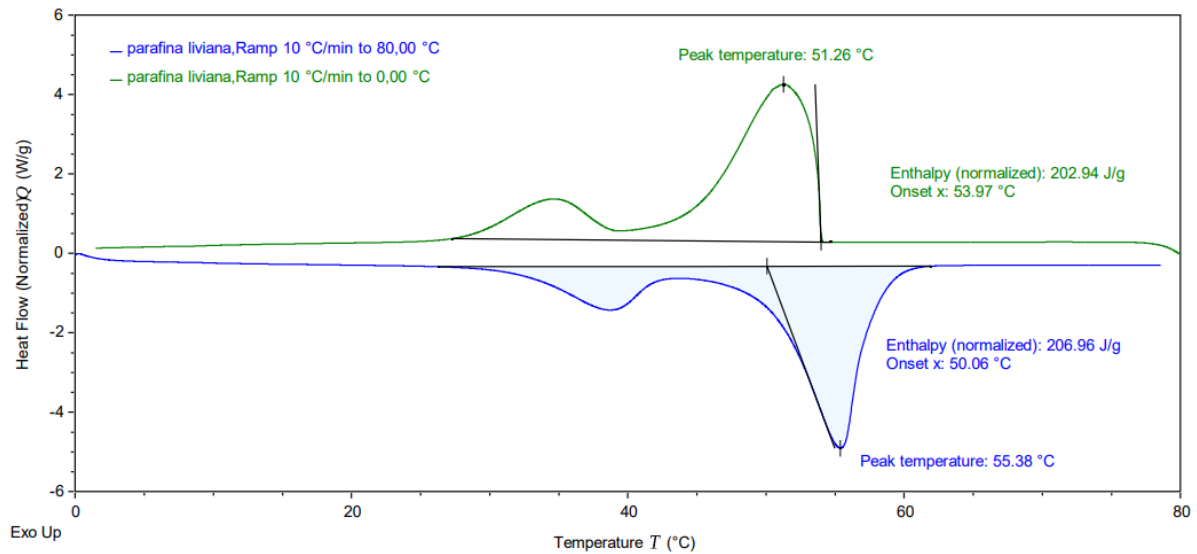


Figure 8. DSC curve performed at 10 °C/min for Light paraffin.

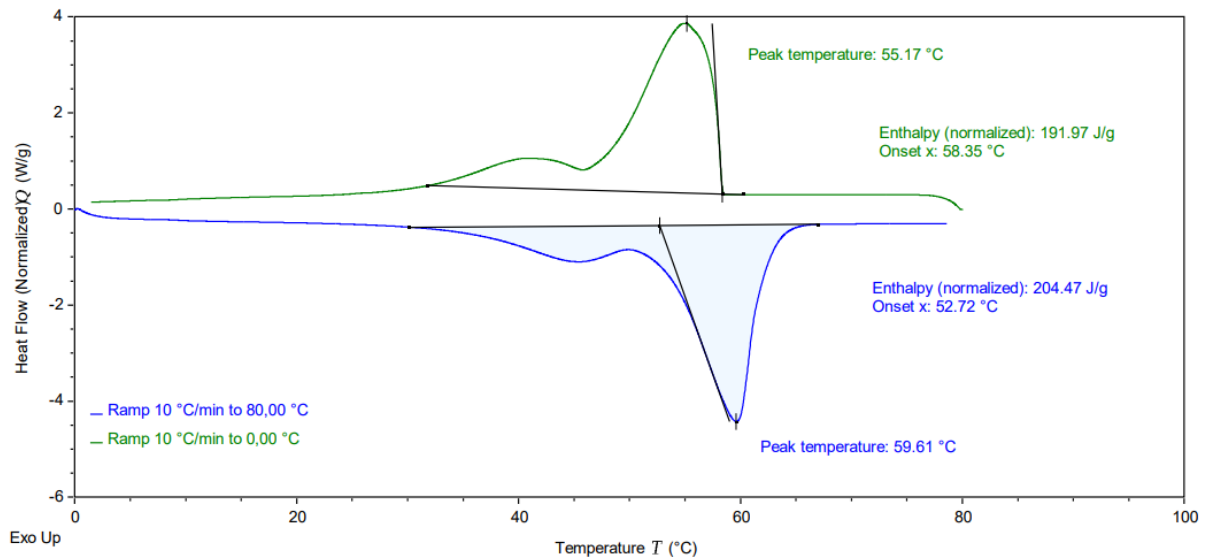
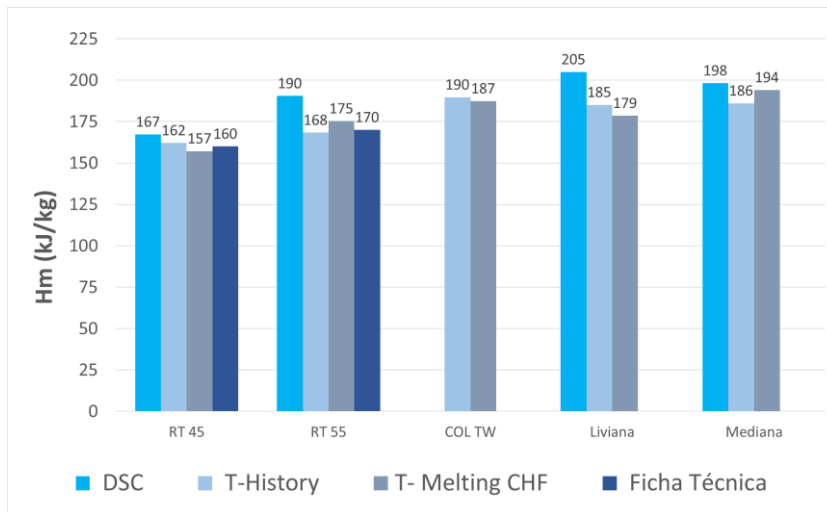


Figure 9. DSC curve performed at 5 °C/min for RT 45 paraffin.

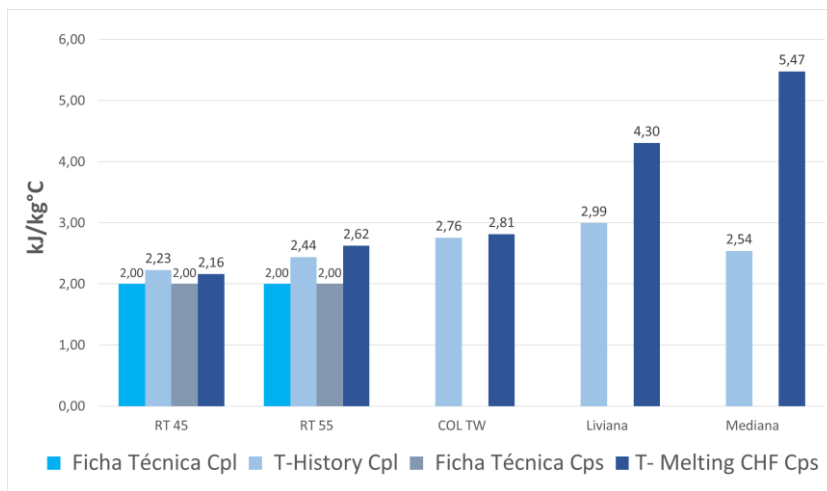
Table 3. Comparison of fusion enthalpy values between the DSC method and those found in the literature.

PCM	Phase Change (°C)		Hm	Hm
	Heating	Cooling	Heating (kJ/kg)	Cooling (kJ/kg)
RT 45	--	42.48	--	167.24
RT 55	--	52.52	--	190.46
Light	55.38	51.26	206.96	202.94
Medium	59.61	55.17	204.47	191.97

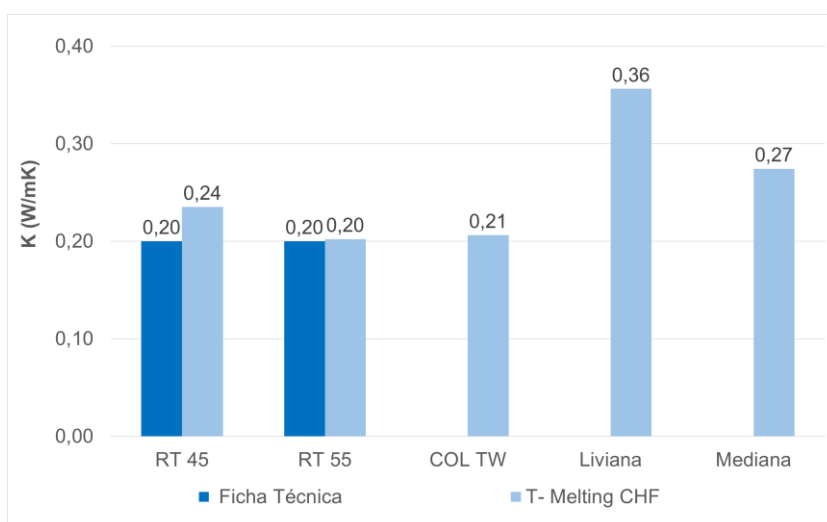
Once the individual analysis of each PCM has been performed using different methods, it is essential to carry out a comparison of the obtained results. For this purpose, the data is presented in different graphs to facilitate visualization and analysis. Graph 1 shows the Fusion Enthalpy (Hm), while Graph 2 displays the values corresponding to the Liquid Specific Heat Capacity (Cpl) and Solid Specific Heat Capacity (Cps). On the other hand, Graph 3 presents the data related to Thermal Conductivity (K). These values are complemented by the information provided in the technical datasheets of RT-45 and RT-55 paraffins. The DSC data shows slightly higher values compared to those reported in the literature, the T-History method also reported higher values compared to those in the literature. In contrast, the T-Melting CHF method recorded values both above and below the reference values.



Graph 1: Fusion Enthalpy (Hm) obtained using the different methods



Graph 2: Liquid Specific Heat Capacity (Cpl) and Solid Specific Heat Capacity (Cps) obtained using the different methods



Gráfica 3: Conductividad térmica (K): Ficha Técnica y método T-Melting CHF

## 4. CONCLUSIONS

Through this research, the main thermophysical properties of three low-cost commercial paraffins were determined. Furthermore, in the search for unconventional methods to determine these properties, it was demonstrated that the T-History and T-Melting CHF methods can be used to evaluate thermal properties.

In the case of the T-History method, difficulties were encountered in estimating Cps due to challenges in accurately evaluating the differences in the area when the reference, environment, and sample have very similar temperatures. As for the T-Melting CHF method, the calculation of Cpl is challenging due to heat losses in the test module.

Since the thermophysical property values of the studied PCMs are close to those reported in international paraffin datasheets, which are used in thermal energy storage systems, it can be concluded that they have potential for thermal energy storage.

Given that the replicated methods require continuous temperature recording of the analyzed samples, it is necessary to ensure a controlled environment and improved thermal insulation in each test device to reduce data noise.

For the T-History method, where only the cooling process of the samples was analyzed, it would be interesting to study the materials during the melting process and compare the results obtained, thus it is recommended to construct a thermal chamber.

On the other hand, in the T-Melting CHF method, the data exhibited high levels of noise, highlighting the need for improved thermal insulation of the test module and an enhanced control system regulating the resistance power.

## 5. ACKNOWLEDGEMENTS

The authors would like to thank the University of Córdoba for the funding provided within the framework of the Sustainability of Research Groups in the Department of Mechanical Engineering, associated with the Engineering, Science, and Technology Group - ICT. They also acknowledge the Master's program in Mechanical Engineering.

## 6. REFERENCES

- Agyenim, F., Hewitt, N., Eames, P., & Smyth, M. (2010). A review of materials, heat transfer and phase change problem formulation for latent heat thermal energy storage systems (LHTESS). *Renewable and Sustainable Energy Reviews*, 14(2), 615–628.
- American, A., & Standard, N. (n.d.). Designation: D 4419-90 (Reapproved 2000) Standard Test Method for Measurement of Transition Temperatures of Petroleum Waxes by Differential Scanning Calorimetry (DSC) 1.
- Dincer, I. On thermal energy storage systems and applications in buildings. (2002). *Energy and Building*, 34(4), 377–388.
- Dumas, J. P., Gibout, S., Zalewski, L., Johannes, K., Franquet, E., Lassue, S., Bédécarrats, J. P., Tittlein, P., & Kuznik, F. (2014). Interpretation of calorimetry experiments to characterise phase change materials. *International Journal of Thermal Sciences*, 78, 48–55.
- Jin, X., Xu, X., Zhang, X., & Yin, Y. (2014). Determination of the PCM melting temperature range using DSC. *Thermochimica Acta*, 595, 17–21.
- Koshti, B., Dev, R., Bharti, A., & Narayan, A. (2023). Comparative performance evaluation of modified solar cookers for subtropical climate conditions. *Renewable Energy*, 209, 505–515.
- Mahdi, J. M., Lohrasbi, S., & Nsofor, E. C. (2019). Hybrid heat transfer enhancement for latent-heat thermal energy storage systems: A review. *International Journal of Heat and Mass Transfer*, 137, 630-649.
- Mayayo, J. *Materiales de Cambio de Fase*. 2012. Diseño de una instalación para la caracterización de PCM a altas temperaturas. Universidad Zaragoza, Ingeniería Técnica Industrial - Especialidad Mecánica.
- Mayilvelnathan, V., & Valan Arasu, A. (2019). Characterization and thermophysical properties of graphene nanoparticles dispersed erythritol PCM for medium temperature thermal energy storage applications. [Thermochemical Acta](#), 676, 94-103.
- Midilli, A., Dincer, B., & Rosen, & M. A. (2007). The Role and Future Benefits of Green Energy. *International Journal of Green Energy*, 4(1), 65–87.
- Peñalosa G, M. C. (2016). Avances en determinación de propiedades termofísicas de materiales de cambio de fase: búsqueda y análisis de nuevos materiales PCM-TES de bajo coste. Universidad de Zaragoza, Departamento de Ingeniería Mecánica.
- Raccanello, J., Rech, S., & Lazzaretto, A. (2019). Simplified dynamic modeling of single-tank thermal energy storage systems. *Energy*, 182, 1154-1172.
- Yang, X.-H., & Liu, J. (2018). A novel method for determining the melting point, fusion latent heat, specific heat capacity and thermal conductivity of phase change materials. *International Journal of Heat and Mass Transfer*, 127, 457-468.
- Zhang Yinping, Jiang Yi. (1999). A simple method, the T-History method, of determining the heat of fusion, specific heat and thermal conductivity of phase-change materials. *Measurement Science and Technology*, 10(3), 201–205.

## **7. RESPONSIBILITY NOTICE**

The authors are the only responsible for the printed material included in this paper.